Reconstruction of the Pressure Profile of LDX High Beta Plasma

M. Mauel, I. Karim, A. Boxer, J. Ellsworth, D. Garnier,
A. Hansen, J. Kesner, and E. Ortiz

Dept. of Applied Physics and Applied Mathematics, Columbia University
Plasma Science and Fusion Center, MIT

ICC 2006, Austin TX

Abstract

Basic considerations for modeling and measuring anisotropic pressure equilibria in LDX are discussed. We compute a least-squares best-fit of a pressure model, introduced previously by Connor-Hastie, to magnetic and x-ray measurements. The anisotropic pressure has four parameters:

(i) The ratio $P_\perp/P_\|$

(ii) The radial location of the peak pressure,

(iii) The radial width of the pressure profile, and

(iv) The plasma diamagnetic current.

To fit this model to the magnetic measurements, the plasma current is related to the pressure through the self-consistent equilibrium. Since the detected signal from a magnetic sensor combines contributions from the plasma current with the decrease of the current required to maintain constant the flux linked by the superconducting dipole, we find equally good fits occur either with steep profiles centered at large radii or with broad profiles centered at smaller radii. These equilibrium profiles have similar plasma dipole moments.

When only single-frequency ECRH is applied, very good fits result for a range of pressure-peak profiles that is resolved using x-ray imaging. Plasma with the highest values of beta and diamagnetic current are created with multiple-frequency heating. The sum of the mean-square deviations between the best-fit model profile and the magnetic measurements doubles as compared with single-frequency heating, and this may be related to the presence of two pressure peaks, one at each resonance. With the pressure profile peak assumed to be midway between the resonances, then 5 kW of heating creates a plasma with 3.5 kA of plasma current, a peak perpendicular pressure of 750 Pa, and a maximum local beta of 21%.

This poster will present details of the reconstruction procedure and describe new magnetic sensors that will achieve improved reconstruction accuracy.

Cluster II

(Launched 16 July 2000)

Measuring Plasma Currents in Space!

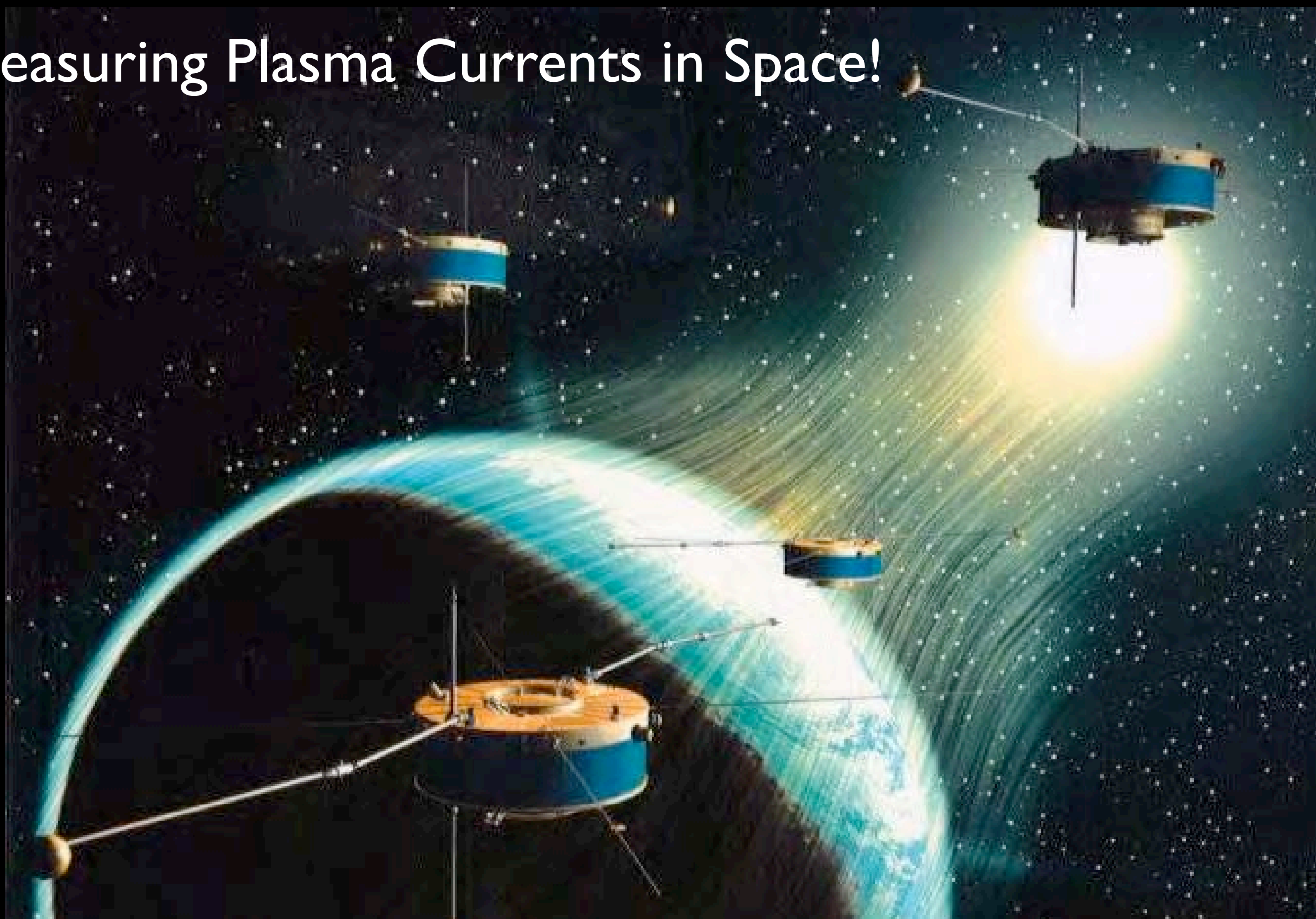

Curlometer

(Vallat, *et al.*, *Annales Geophys,* 2005)

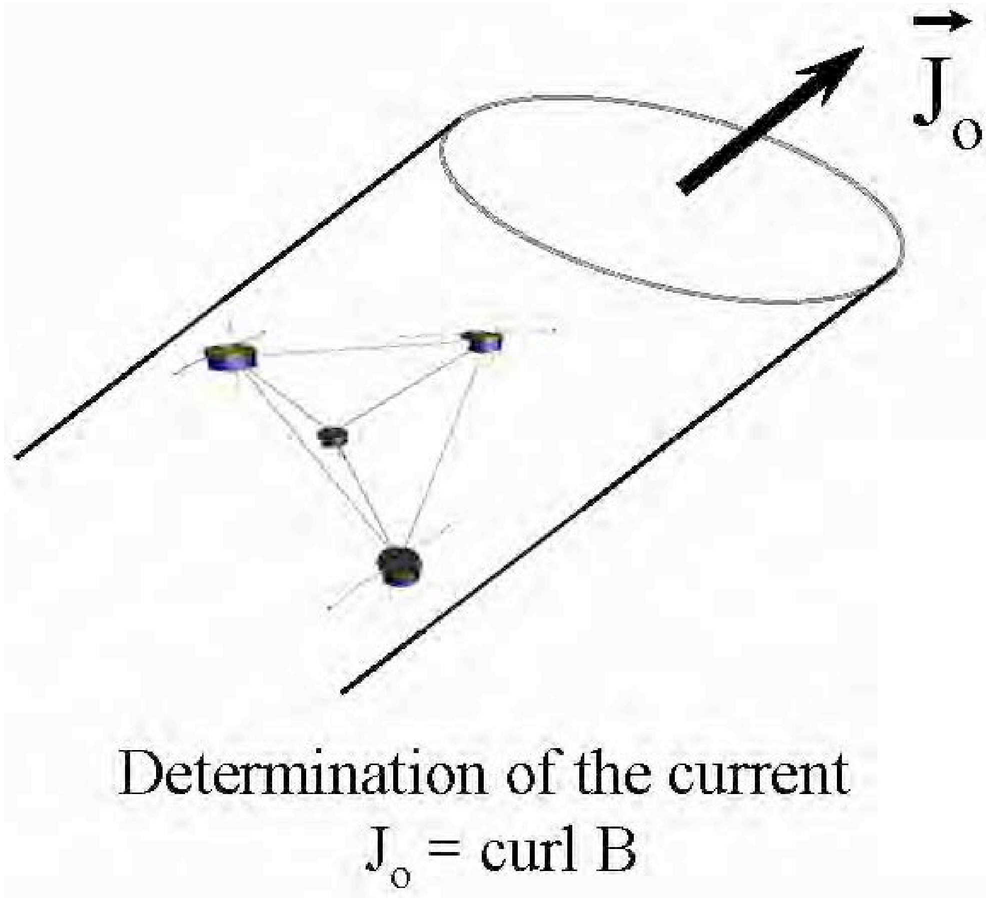

$$\mathbf{J}_\perp = \frac{\mathbf{B} \times \nabla P_\perp}{B^2} + \frac{\mathbf{B} \times \kappa}{B^2}(P_{||} - P_\perp)$$

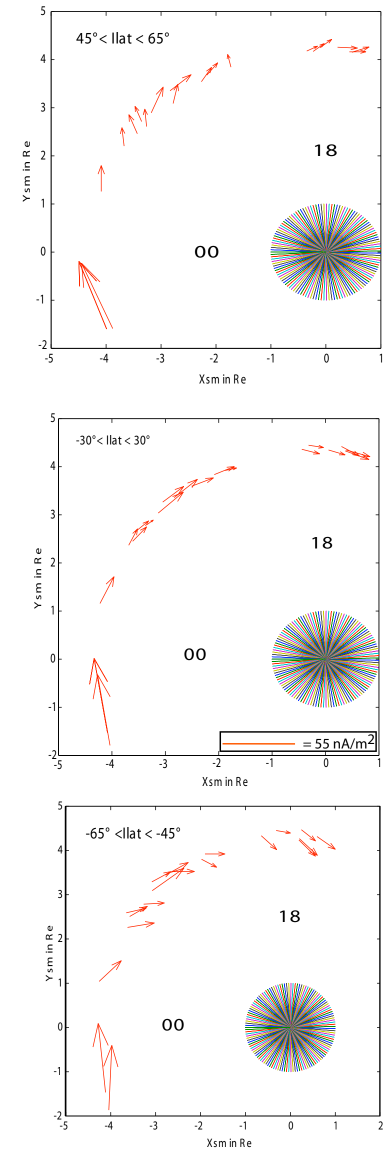

Fig. 15. Current density vectors for the February-June 2002 Cluster perigee passes, averaged over three invariant latitude intervals, and projected down to the equatorial plane: (**a**) from 45° to 65° (**b**) from −30° to 30° (**c**) from −45° to −65°

Ring Current:
Trapped, High-β Protons (15-250 keV)

- Greatly intensified during geomagnetic storms
- $T_i \sim 7T_e$ and $P_\perp \sim 1.5\, P_{||}$
- Monthly storms: ~5 MA. (LDX: 3-4 kA) 10 MA storms few times a year.
- Current centered near $L \sim 4\text{-}5R_e$; $\Delta L \sim 2.6R_e$ wide and $\Delta z \sim 1.6R_e$; *Not axisymmetric.*
- Curlometer during storms: $J_{RC} \sim 25$ nA/m^2 (Cluster II, 2005)

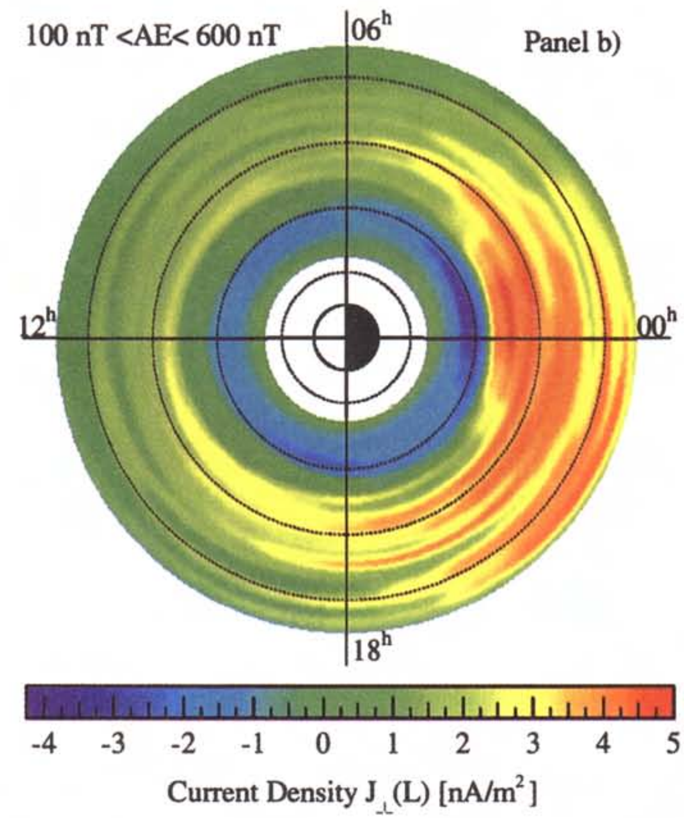

AMPTE/CCE-CHEM Measurements
Averaged over 2 years
(De Michelis, Daglis, Consolini, *JGR*, 1999)

D_{st} and the Dessler-Parker-Sckopke Relation

- Disturbed Storm Time Index (D_{st}):

  $\Delta B_H = (\mu_0/2) \times I_{RC}/R_{rc}$
  measured near equator
  plus Earth's induction fields!
  (LDX: $\Delta I_F \approx -0.25\ I_{rc}$)

- Dessler-Parker-Sckopke:

  Energy = 0.54 GJ/A × I_{RC}
  (LDX: 0.12 J/A)

(Burton, McPherron, Russell, *JGR*, 1975)

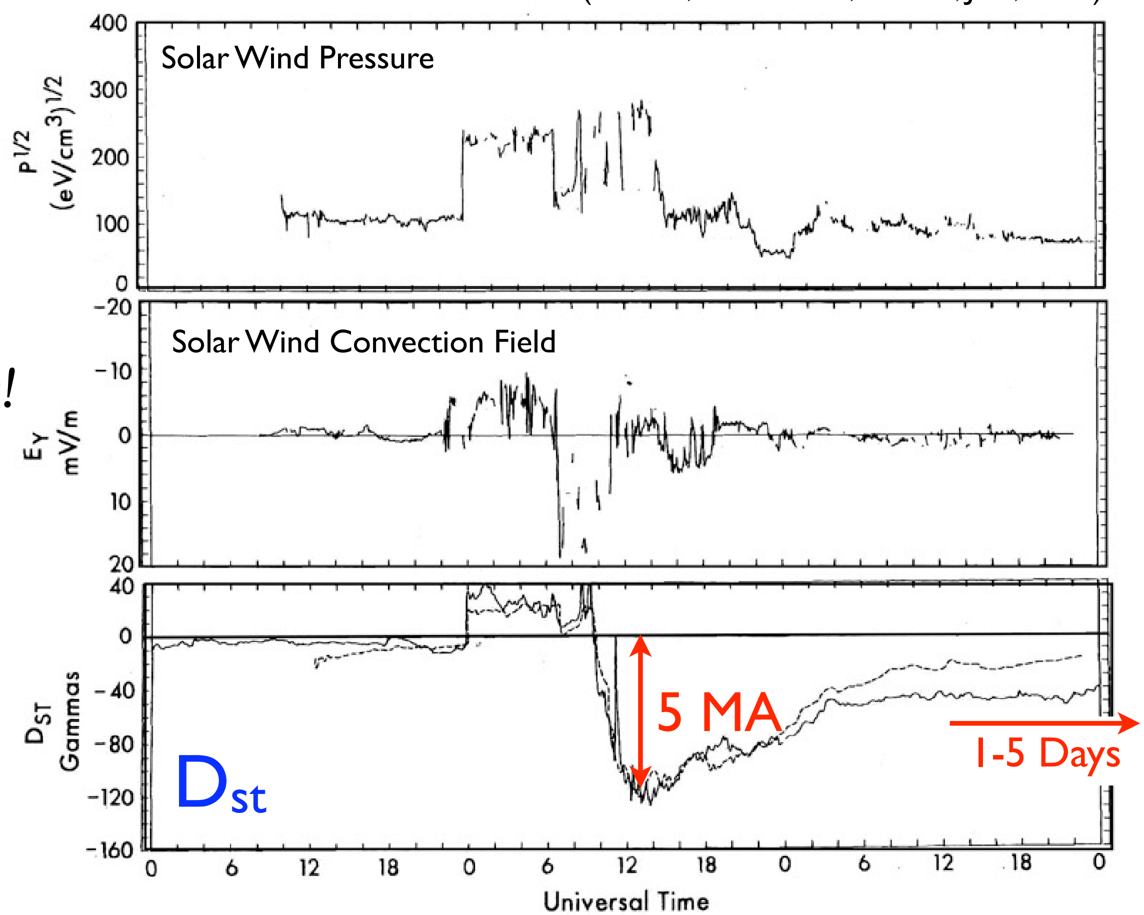

Centrally-Peaked Proton Pressure (Even with Plasma Sheet, Outer-Edge, Source!)

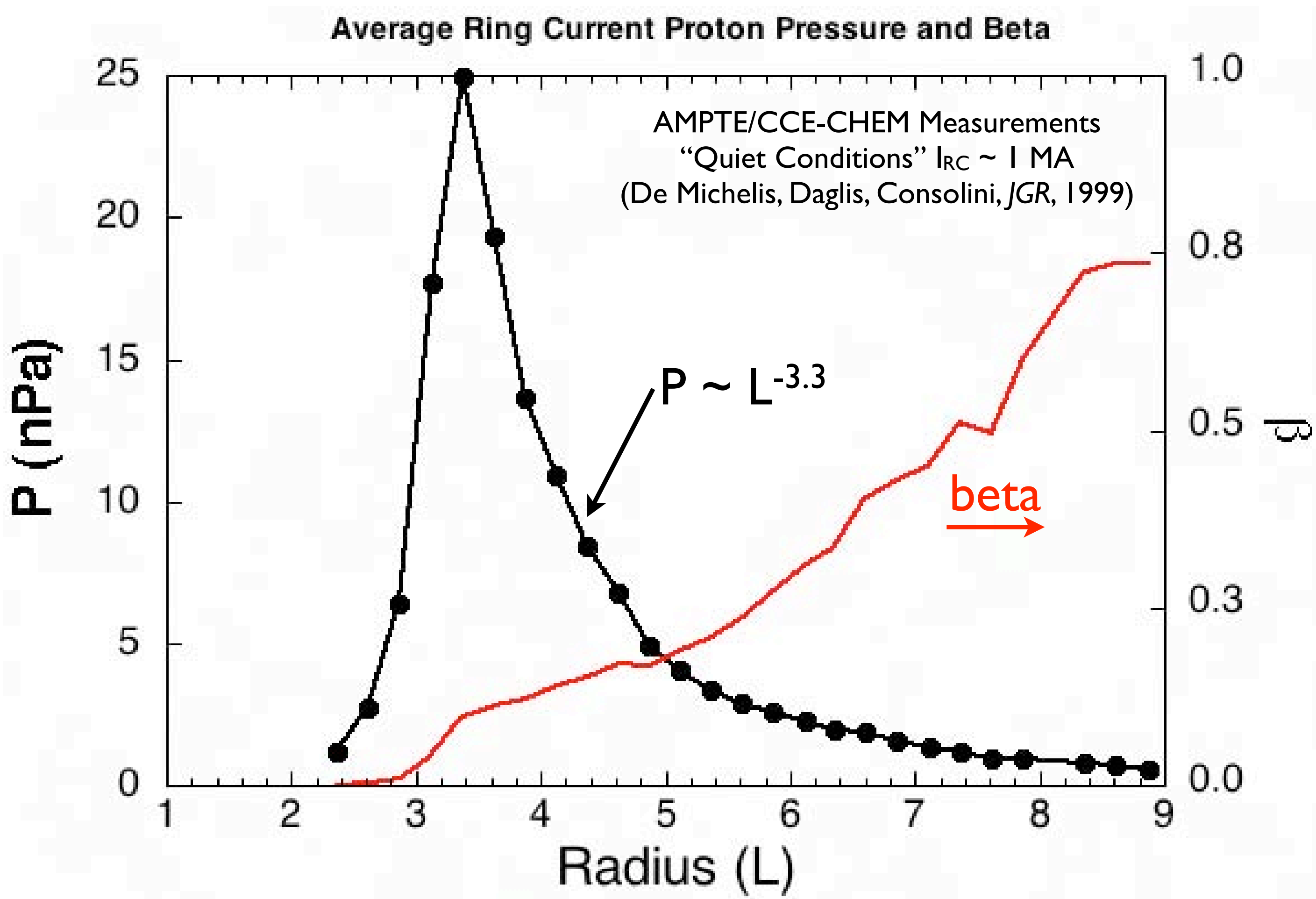

Earth

Magnetic Sensors

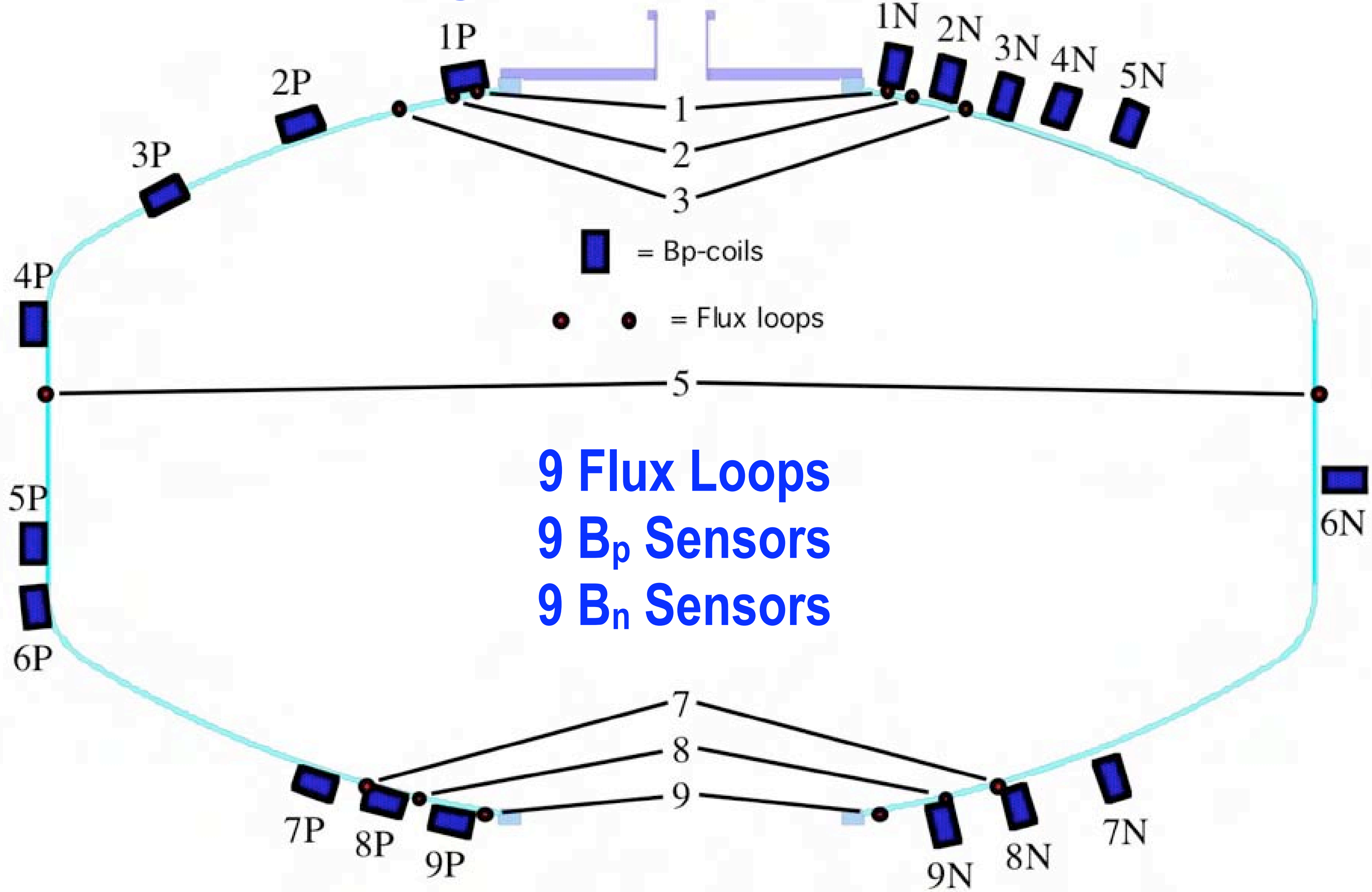

Flux Loop:

- Measures magnetic flux.
- Signal is integrated.
- +/- 0.1 mV·s estimated error

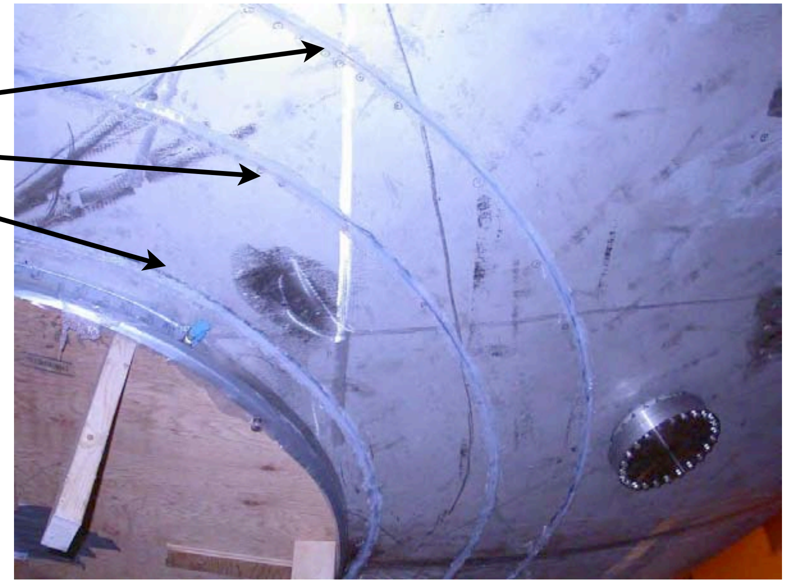

Sensors that measure magnetic field and flux.

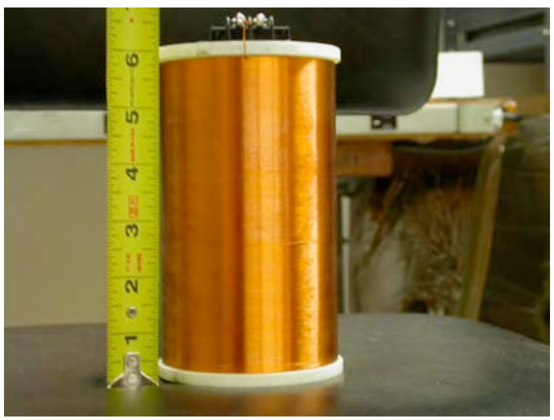

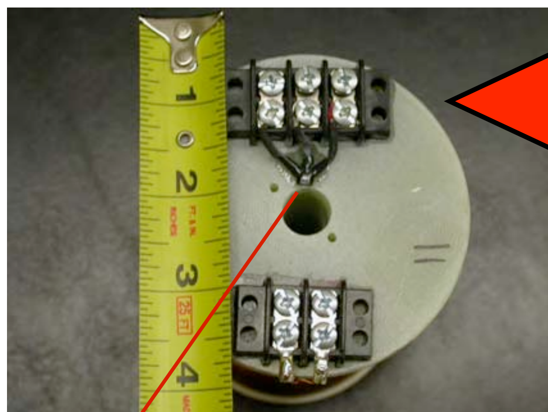

B_p Coils and Hall Sensors

B_p-Coil Specs:
- NA ~ 5 m^2
- Sensitivity: 500 mV/G (connected to a 1 ms RC integrator)
- +/- 0.1 G estimated error

Hall Probe

Hall Sensor Specs:
- Field Range: +/- 500 G
- Sensitivity: 5 mV/G

B_p, B_n Sensors Installed

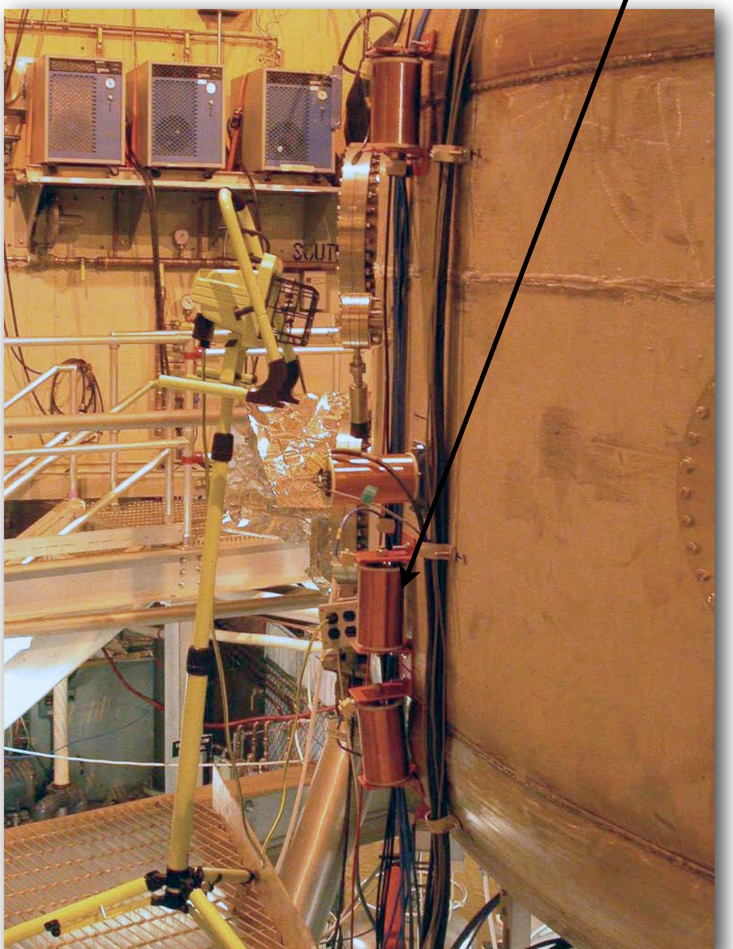

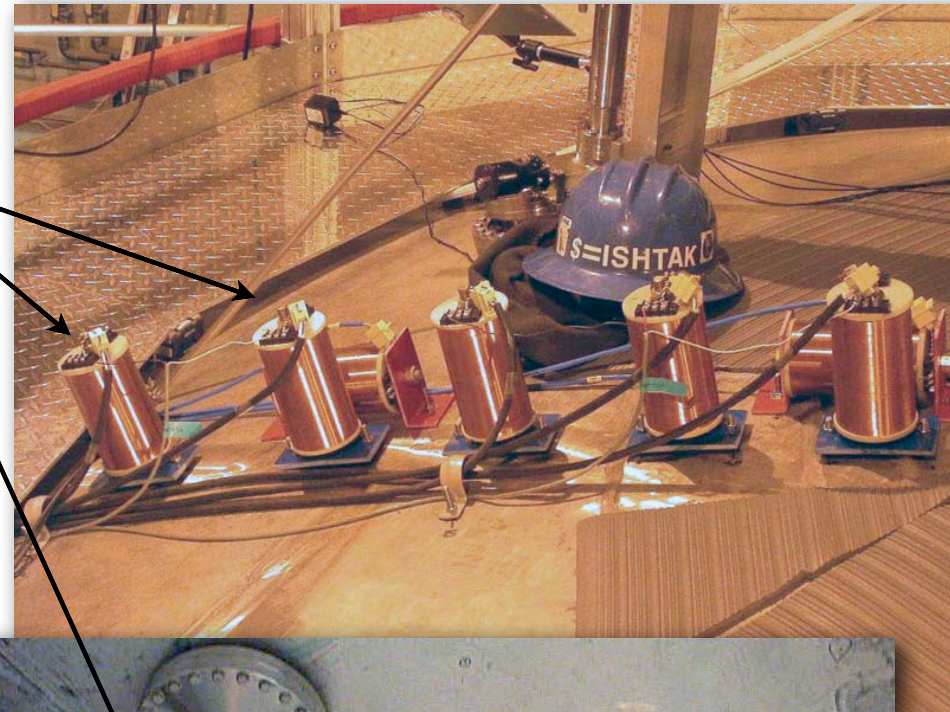

Anisotropic Equilibria

The equilibrium equations are

$$
\begin{aligned}
\mathbf{J} \times \mathbf{B} &= \nabla \cdot \mathsf{P} && (1)\\
\nabla \times \mathbf{B} &= \mu_0 \mathbf{J} && (2)\\
\nabla \cdot \mathbf{B} &= 0 && (3)\\
\mathsf{P} &= P_\perp \mathsf{I} + (P_{||} - P_\perp)\mathbf{bb} && (4)
\end{aligned}
$$

where $\mathbf{B} = B\mathbf{b}$. Free-boundary, high-beta equilibria have been reconstructed with *isotropic* pressure. But, with anisotropic pressure, only free-boundary, low-beta, equilibria have been reconstructed.

The parallel force condition is $\mathbf{B} \cdot \mathbf{J} \times \mathbf{B} = 0$. This implies

$$
\begin{aligned}
\frac{\partial P_{||}}{\partial B} &= (P_{||} - P_\perp)/B && (5)\\
\frac{\partial P_{||}}{\partial s} &= (P_{||} - P_\perp)\frac{d \ln B}{ds} && (6)
\end{aligned}
$$

Equilibrium Current

The perpendicular force balance is given by

$$\mathbf{J} = \frac{\mathbf{B} \times \nabla \cdot \mathsf{P}}{B^2}\,. \tag{7}$$

Perpendicular force balance determines the equilibrium diamagnetic current density. The right-hand-side of Eq. 7 gives

$$\begin{aligned} \mathbf{B} \times \nabla \cdot \mathsf{P} &= \mathbf{B} \times \nabla P_\perp + \mathbf{B} \times \nabla \cdot [\mathbf{bb}(P_{||} - P_\perp)] \\ &= \mathbf{B} \times \nabla P_\perp + (P_{||} - P_\perp)\, \mathbf{B} \times \kappa \end{aligned}$$

where $\kappa = \mathbf{b} \cdot \nabla \mathbf{b}$ is the magnetic curvature. The plasma diamagnetic current is

$$\mathbf{J} = \frac{\mathbf{B} \times \nabla P_\perp}{B^2} + \frac{\mathbf{B} \times \kappa}{B^2}\,(P_{||} - P_\perp) \tag{8}$$

Vacuum Fields

With about 1 MA·turn flowing in the LDX floating coil and only a few kA in the plasma, the magnetic fields in the present-day LDX discharges are very nearly equal to the vacuum fields. In this case, the magnetic curvature is approximately

$$\kappa = -\mathbf{b} \times \nabla \times \mathbf{b} = -\mathbf{b} \times \left[\frac{1}{B} \nabla \times \mathbf{B} - \mathbf{B} \times \nabla \left(\frac{1}{B} \right) \right] \approx \frac{\nabla_\perp B}{B}$$

since $\nabla \times \mathbf{B} \approx 0$.

Writing $\mathbf{B} = \nabla \phi \times \nabla \psi / 2\pi = \nabla \chi$ (note: 2π!), Eq. 8 can be re-written as

$$J_\phi = -2\pi r \frac{D P_\perp}{D\psi} - 2\pi r (P_{||} - P_\perp) \frac{D \ln B}{D\psi}, \tag{9}$$

where cylindrical coordinates were used to give $|\nabla \phi| = 1/r$ and $D/D\psi \equiv |\nabla \psi|^{-2} \nabla \psi \cdot \nabla$.

Notice that the peak of the (perpendicular) plasma pressure no longer corresponds to a null in the plasma current. Notice also that, when $P_\perp \gg P_{||}$, the plasma current outside the pressure peak is *reduced* relative to the current that would occur with the same level of isotropic pressure.

Model Profiles

In our previous reconstructions of LDX equilibria, we used the model (isotropic) pressure profile

$$p(\psi) = G(\psi) \equiv p_0 \left(\frac{\psi - \psi_{fcoil}}{\psi_0 - \psi_{fcoil}} \right)^{\alpha} \left(\frac{\psi}{\psi_0} \right)^{4g} , \qquad (10)$$

where $\alpha = 4g(|\psi_{fcoil}/\psi_0| - 1)$ and ψ_0 is the value of the poloidal flux at the pressure peak. The pressure profile vanishes at the inner (f-coil) limiter, but it does not vanish at the outer plasma limiter. The variation of G with ψ is

$$\frac{dG}{d\psi} = 4g\, G(\psi) \frac{(\psi_f/\psi_0) - (\psi_f/\psi)}{\psi - \psi_f} .$$

For anisotropic pressure, the equilibrium pressure profile can be characterized by a function of two variable, $(\psi,\ B)$. The simplest models define the pressure as the product of two functions, $P_\perp = G(\psi)H(B(\psi,\chi))$, where $H(B)$ is a function of the magnetic field strength. As B increases toward the dipole's poles, H decreases.

Anisotropic Form (I)

Since $B(\psi,\ \chi)$ is not a flux function, the operator $\partial/\partial\psi$ acts on both $G(\psi)$ and $H(B)$. The plasma current is expressed as

$$J_\phi = -2\pi r \left(H\frac{dG}{d\psi} + GB\frac{dH}{dB}\frac{\partial \ln B}{\partial\psi} \right) - 2\pi r(P_{||}(\psi, B) - GH)\,\frac{\partial \ln B}{\partial\psi}\,. \tag{11}$$

In these reconstructions, we use the much simpler and easier-to-use model employed by Krasheninnikov (2000) and by Simakov (2000). Define the ratio, $H(B) \equiv (B_0/B)^{2p} = (B(\psi,\ \chi = 0)/B(\psi,\ \chi))^{2p}$, to be the ratio of the strength of the field at the equator, B_0, to the strength at a location χ, or s, from the equator. $H(B)$ has a value of unity at the equator that decreases monotonically along the field line towards the floating coil. The pressure *always* peaks on the equatorial plane, even when the ECRH resonance is located near the poles. The parallel pressure is $P_{||} = P_\perp/(1 + 2p)$. When $p > 0$, the plasma is anisotropic.

Anisotropic Form (II)

The gradient of the pressure is

$$\frac{\partial P_\perp}{\partial \psi} = H \frac{dG}{d\psi} + 2pGH \frac{D}{D\psi}(\ln B_0 - \ln B)$$

A convenient expression for the plasma current is

$$J_\phi = -2\pi r H \frac{dG}{d\psi} - 2\pi r G H \frac{2p}{1+2p} \left[2(1+p) \frac{D \ln(B_0/B)}{D\psi} - \frac{\partial \ln B_0}{\partial \psi} \right] \tag{12}$$

where $\partial \ln B_0 / \partial \psi$ is a flux function but $D \ln B / D\psi$ and $D \ln(B_0/B)/D\psi$ are not.

The pressure and current profiles of anisotropic equilibria are illustrated in the next figures when the pressure profile is modeled using the simple model of Connor and Hastie (1976). Relative to isotropic plasmas, anisotropic pressure generates a smaller equilibrium current for the same value of peak pressure.

Anisotropy Significantly Changes Pressure Profile Height

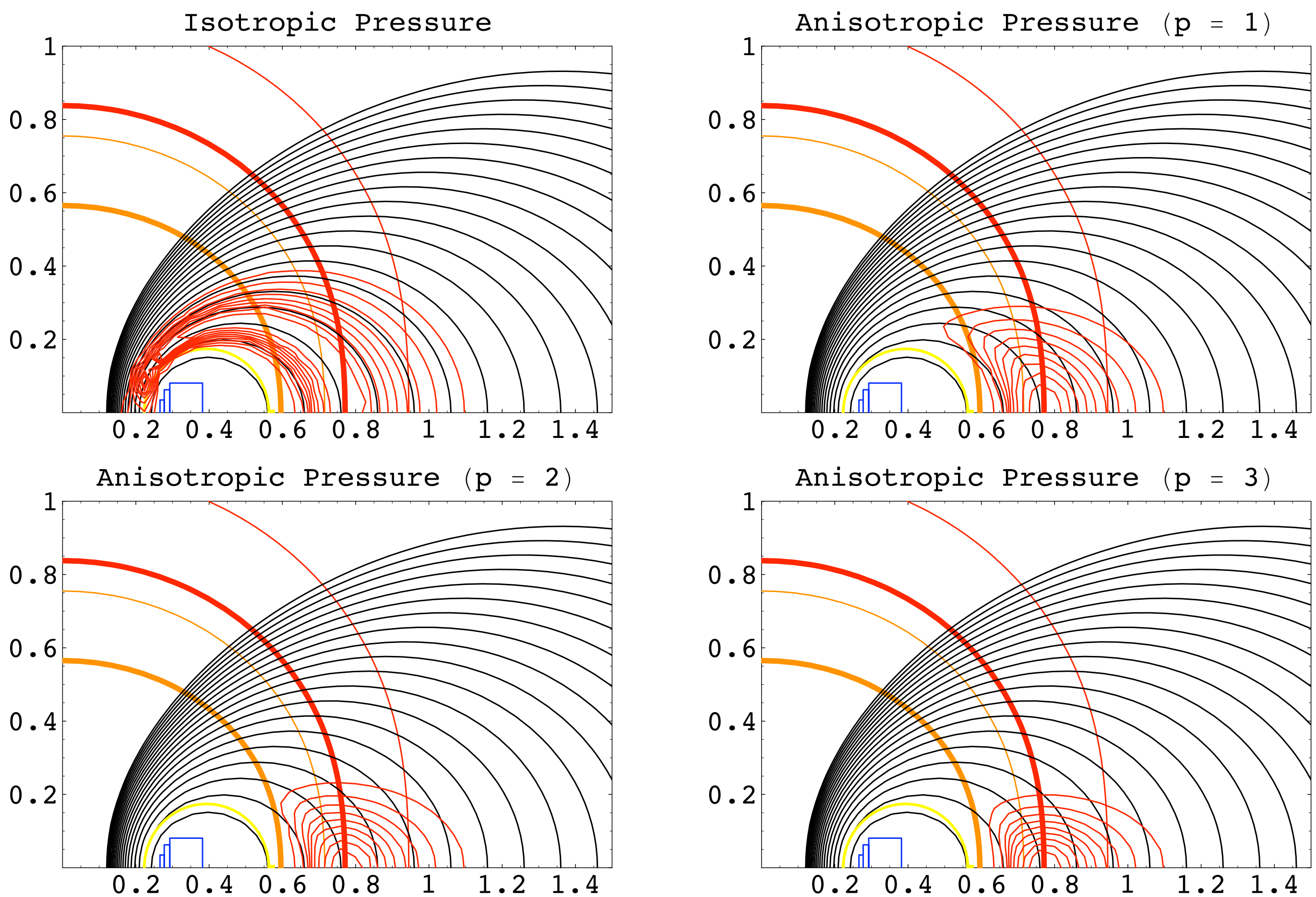

Figure 1: Example anisotropic pressure profiles with $G(\psi)$ defined with $g = 4$ and ψ_0 located at $r = 0.77$ m. The anisotropy parameter was $p = 0$, 1, 2, and 3.

Plasma Current Decreases for Anisotropic Pressure

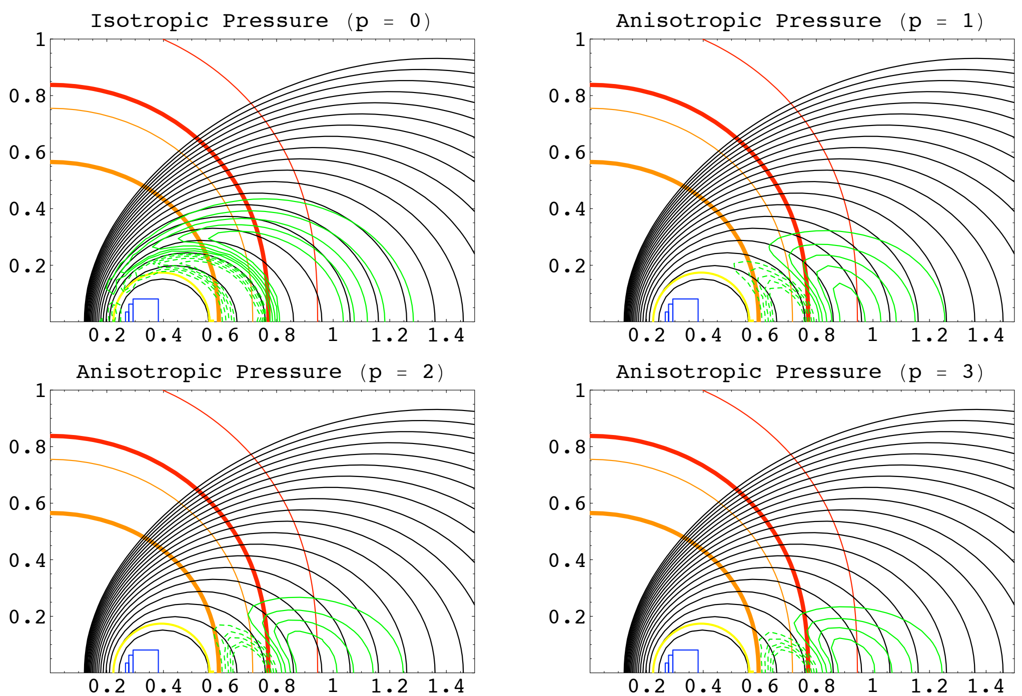

Figure 2: Plasma current profiles for the four pressure profiles shown in Fig. 1.

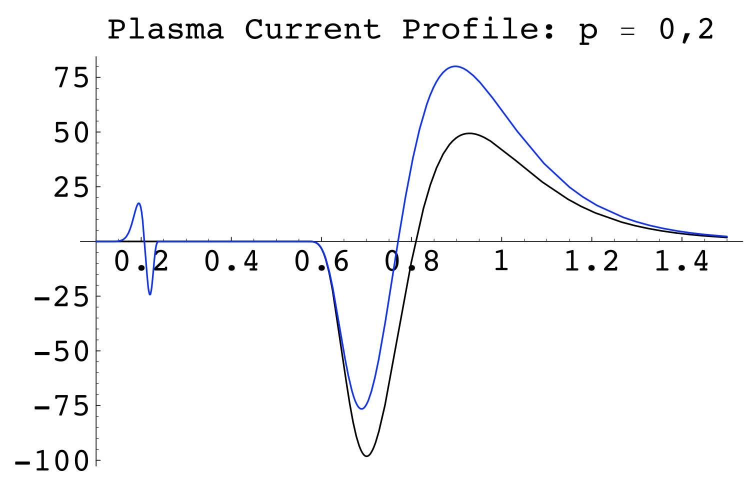

Figure 3: The equatorial plasma current profile when $p = 0$ (blue) and $p = 2$.

Mutual Inductance between Floating Coil and Plasma

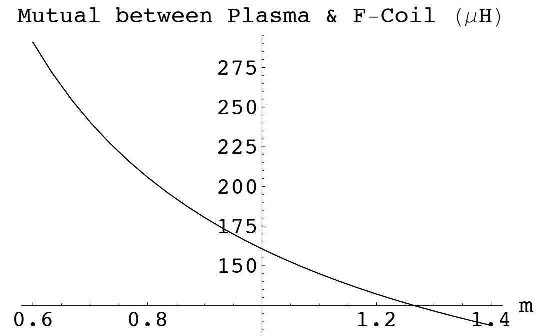

Figure 1: The mutual inductance between the F-coil and an equatorial plasma filament at radius x.

The mutual inductance between the plasma and the floating coil is calculated by performing the following sum and integral:

$$M_{fp} I_p = \int\int \sum_{i=1}^{N} M_i(x,z) J(x,z)\, dx dz \tag{1}$$

where $M_i(x,z)$ is the mutual inductance between a plasma current element at $J(x,z)$ and the ith turn of the F-coil. I_p is the total plasma current. Fig. 1 shows the variation of total mutual inductance, $\sum_i M_i(x,0)$, for a plasma current filament at radius x.

Given the F-coil self-inductance, L_f, the change in the F-coil current is given by the equation for flux conservation:

$$\Delta I_f = -M_{fp} I_p / L_f \tag{2}$$

Table 1: Summary equilibria examples.

	Example1	Example2
Plasma Current (kA)	2.97	2.97
Change in F-Coil Current (kA·turns)	-0.61	-0.76
M_{fp} (μH)	110	138
Current Centroid (m)	1.28	0.96
R(P_{max}) (m)	0.797	0.797
Plasma Volume (m^3)	30.6	30.3
Stored Energy (J)	258	368
$\langle\beta\rangle$	0.370	0.088
β_{max}	0.95	0.62

$$\Delta I_f \approx - I_p/4$$

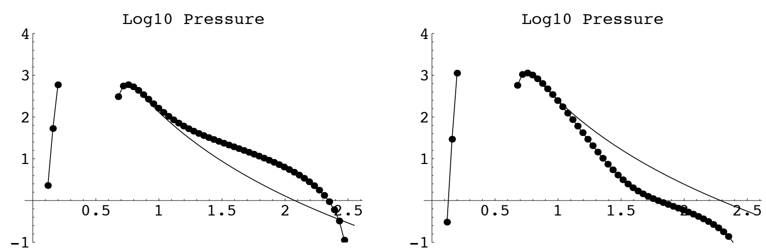

Figure 2: Plots of the $\log_{10} P$ for the two example equilibria. Example 1 is on the left and Example 2 is on the right. The equilibria are shown with the "dots". A thin line scaling with radius as $R^{-20/3}$ is shown for reference.

X-Ray Measurement of Fast Electrons Constrain Equilibrium

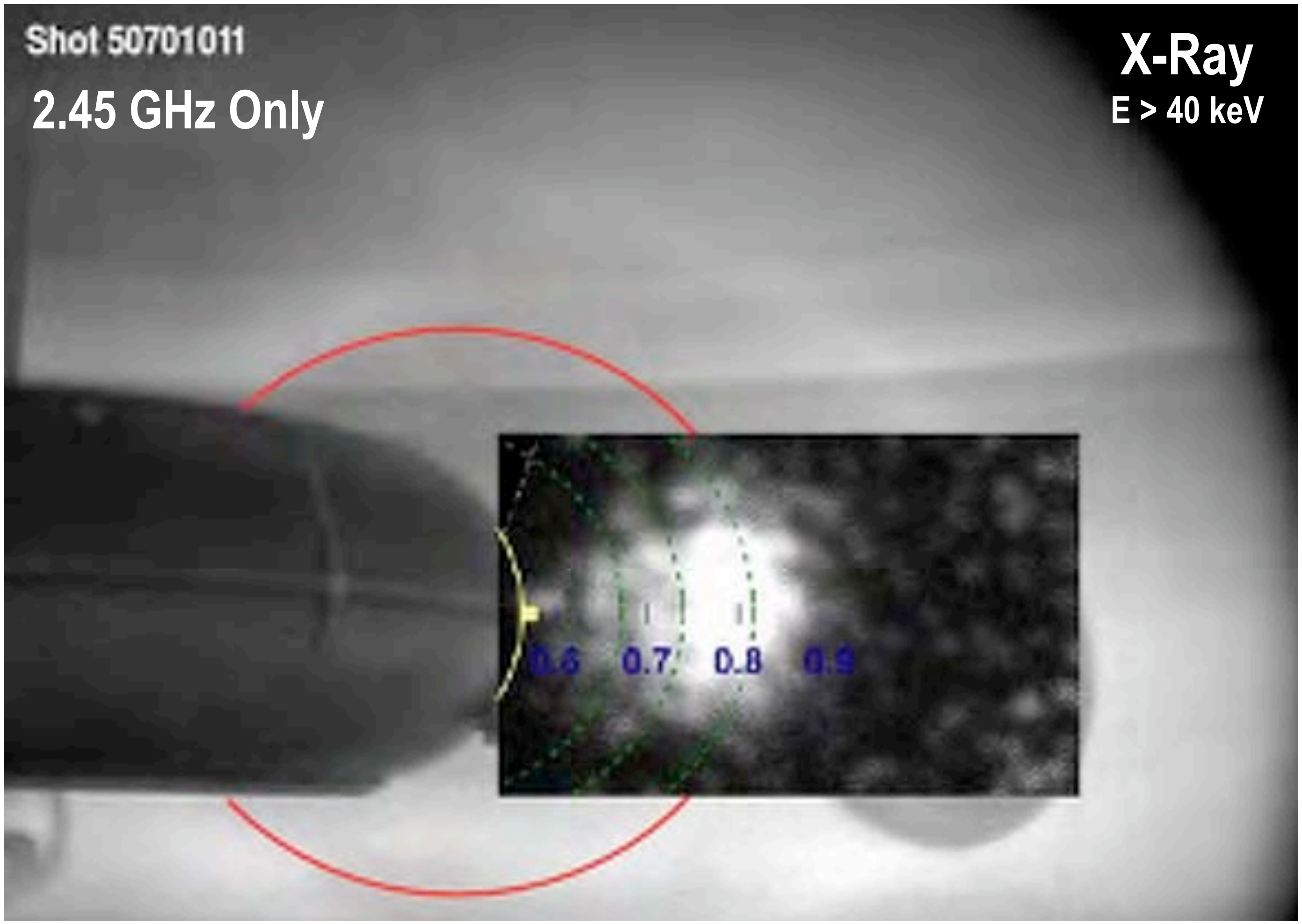

X-Ray Measurement of Fast Electrons Constrain Equilibrium

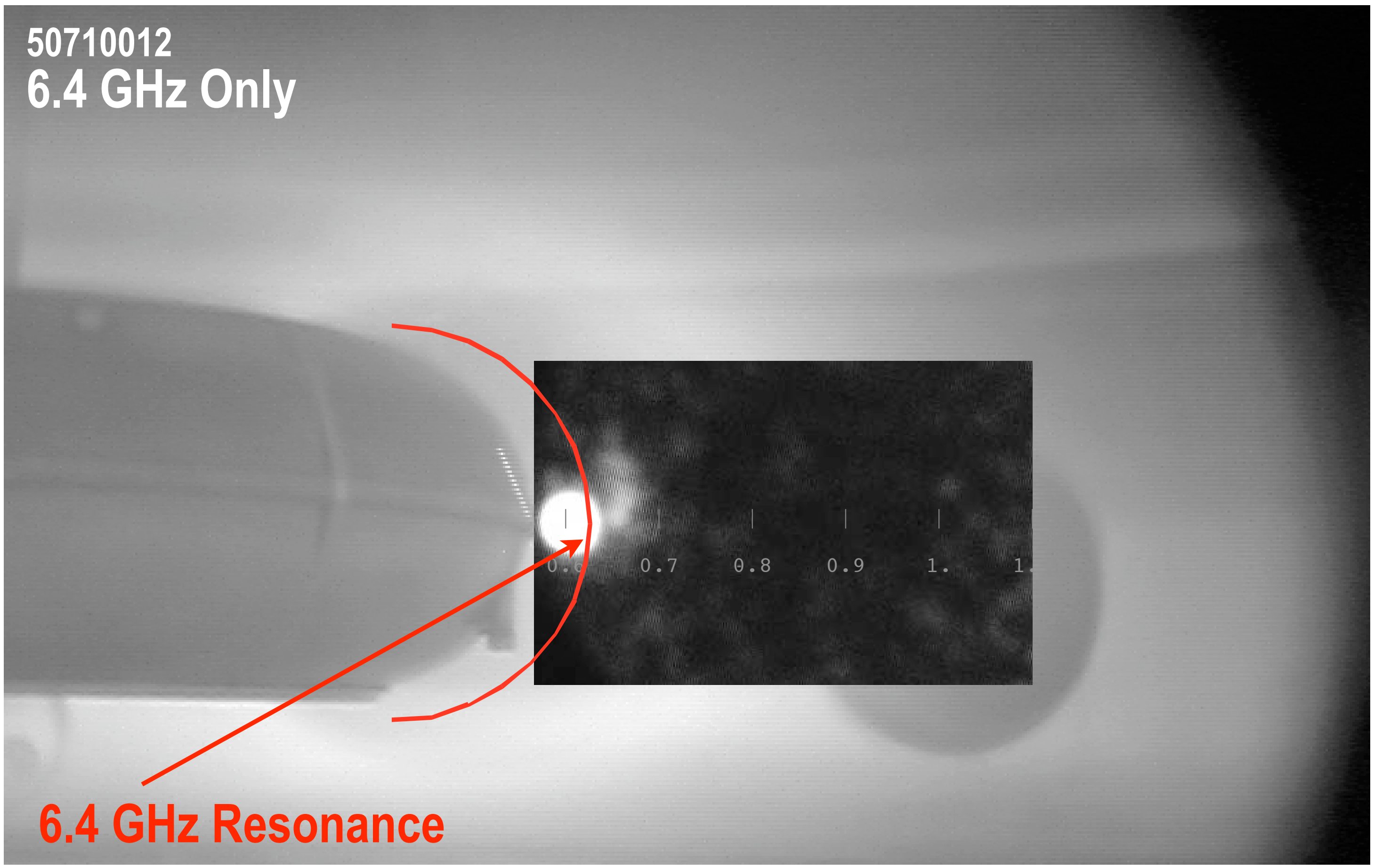

Magnetic Measurements Only **Weakly** Constrain Profiles

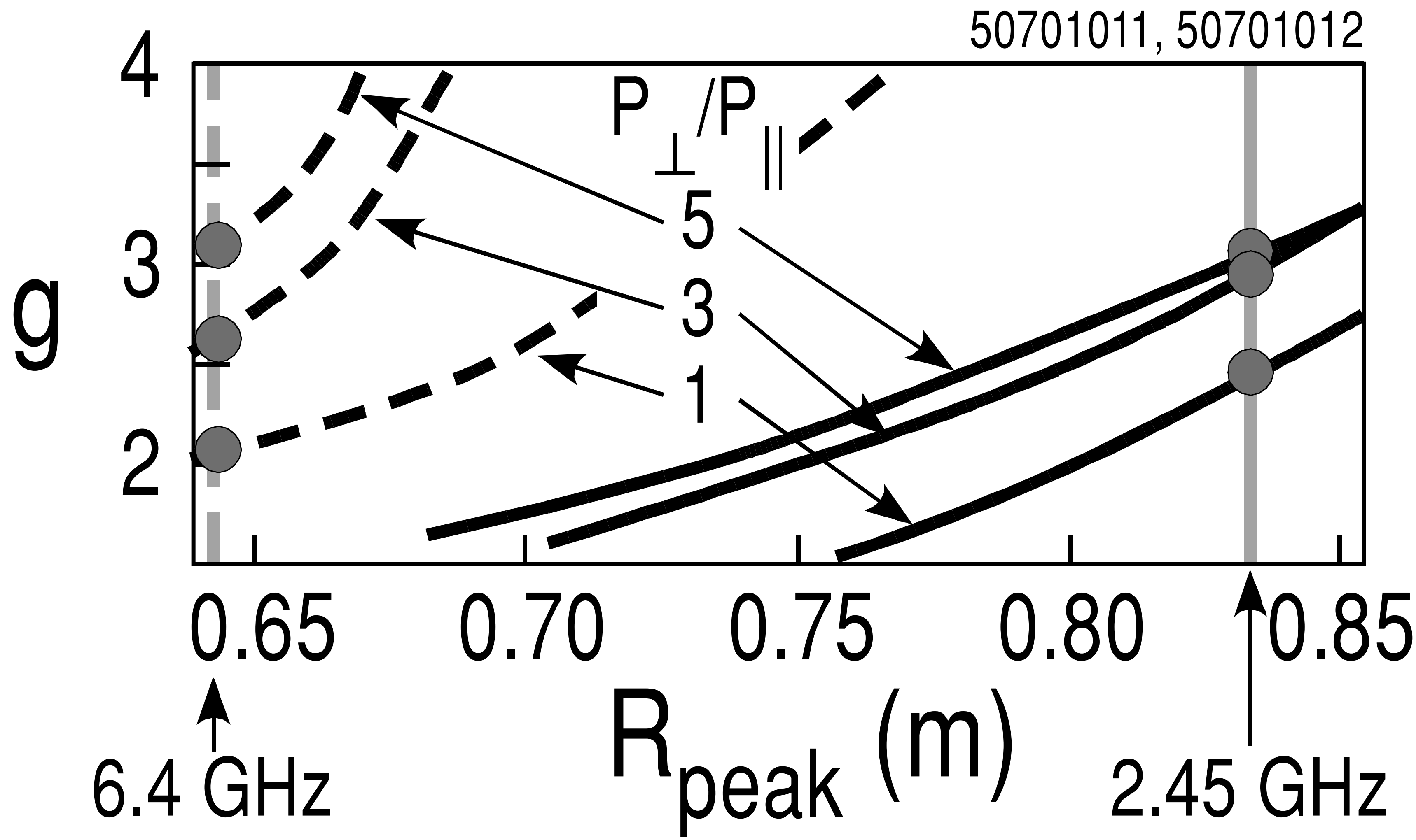

Best Fit Equilibrium for (2.45 GHz) Single-Frequency Heating

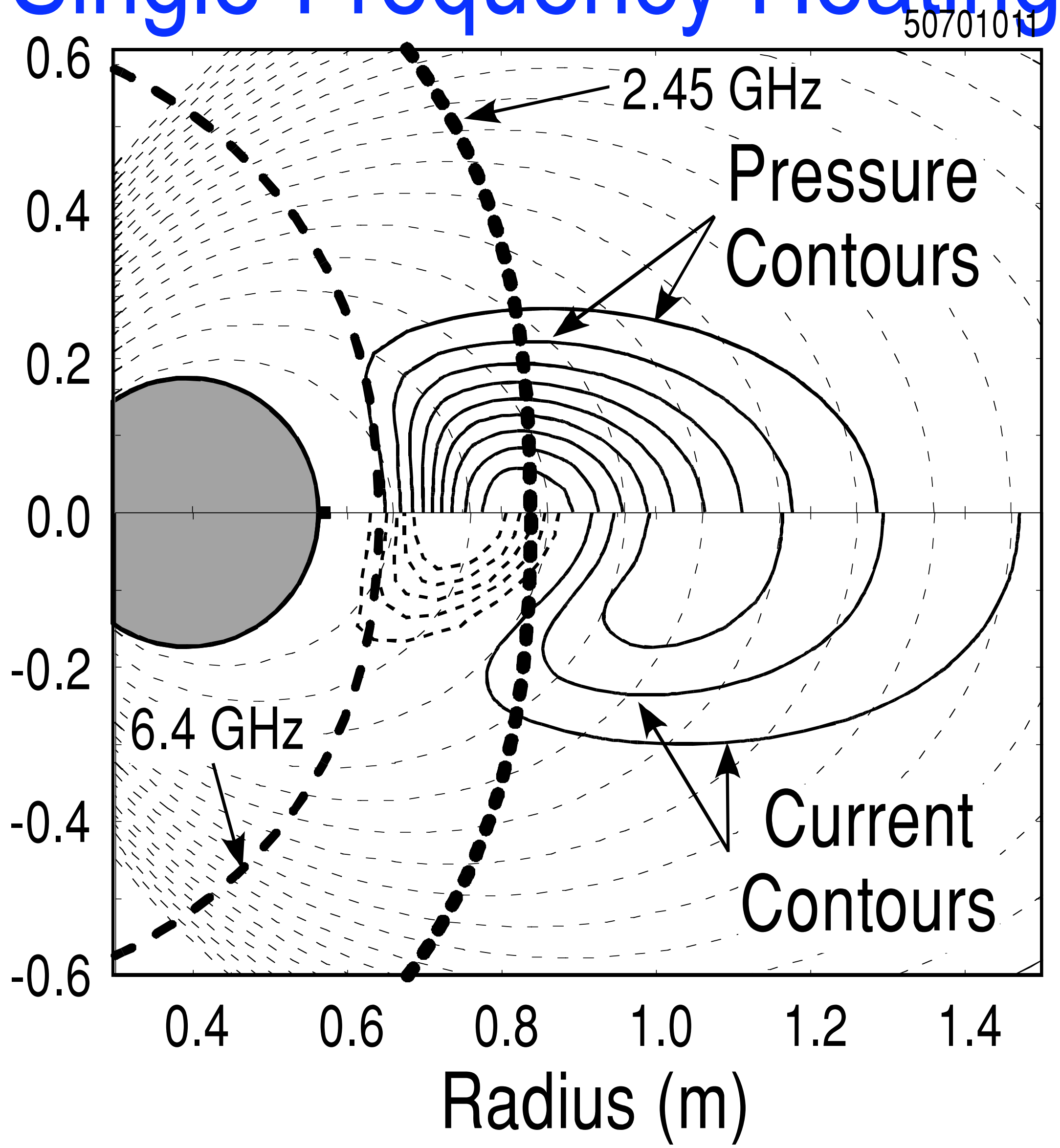

Fit Summary (2.45 GHz Only)

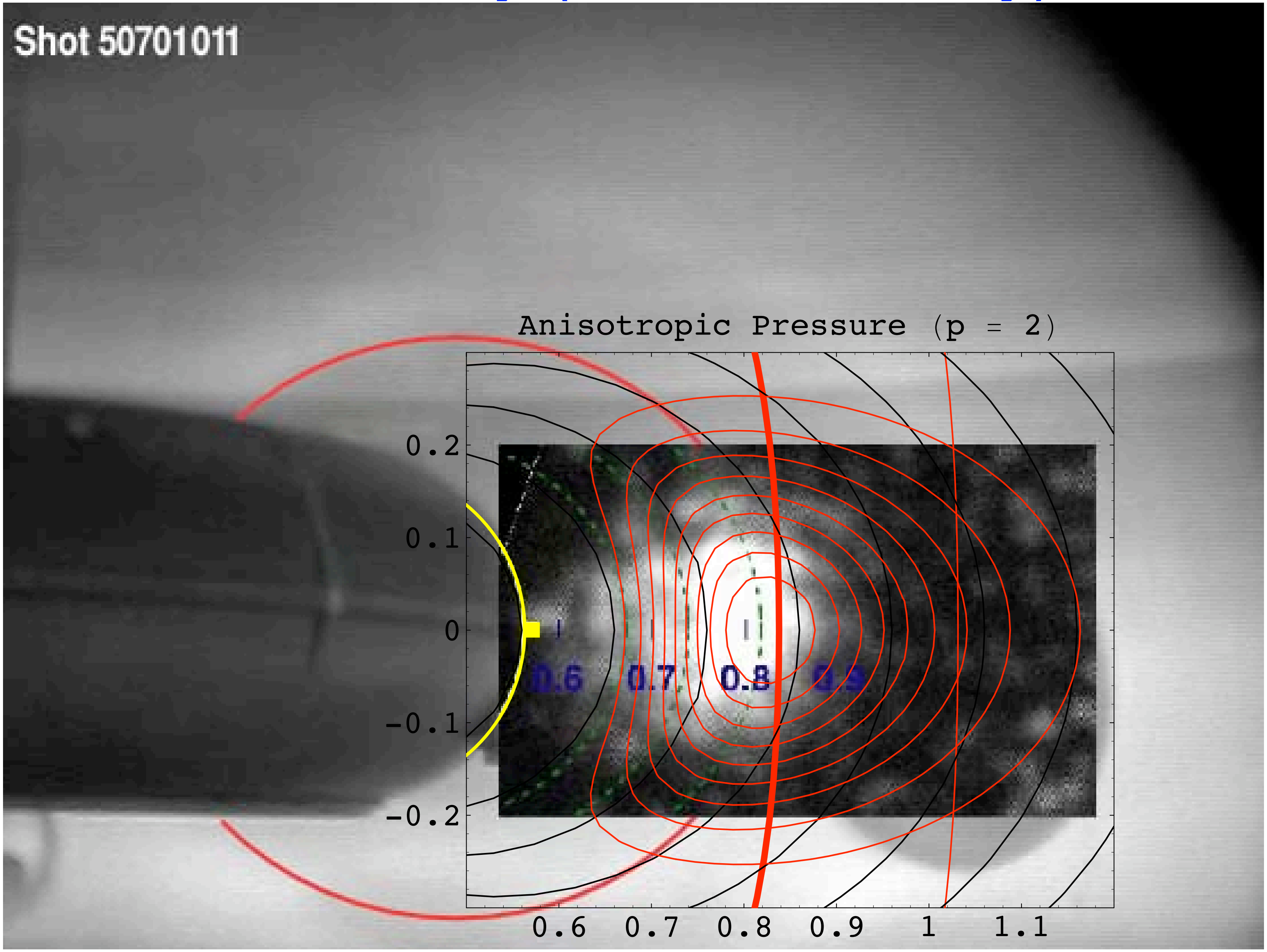

X-Ray Measurement of Fast Electrons Constrain Equilibrium

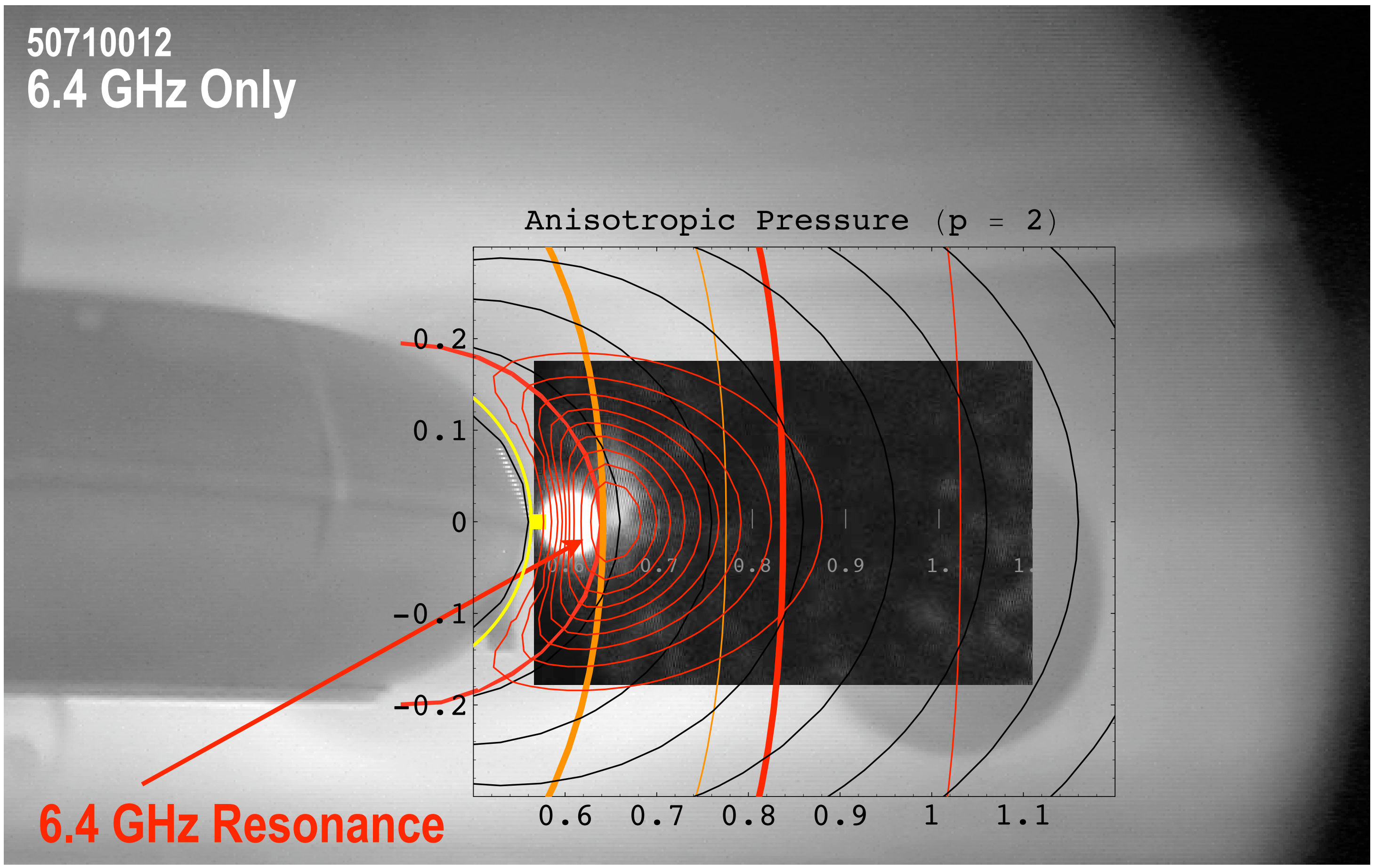

Abel Inversion "Consistent" with Reconstruction

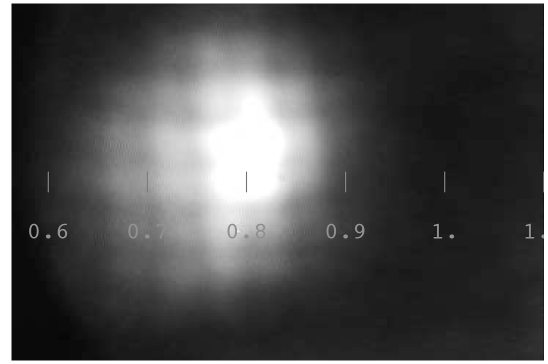

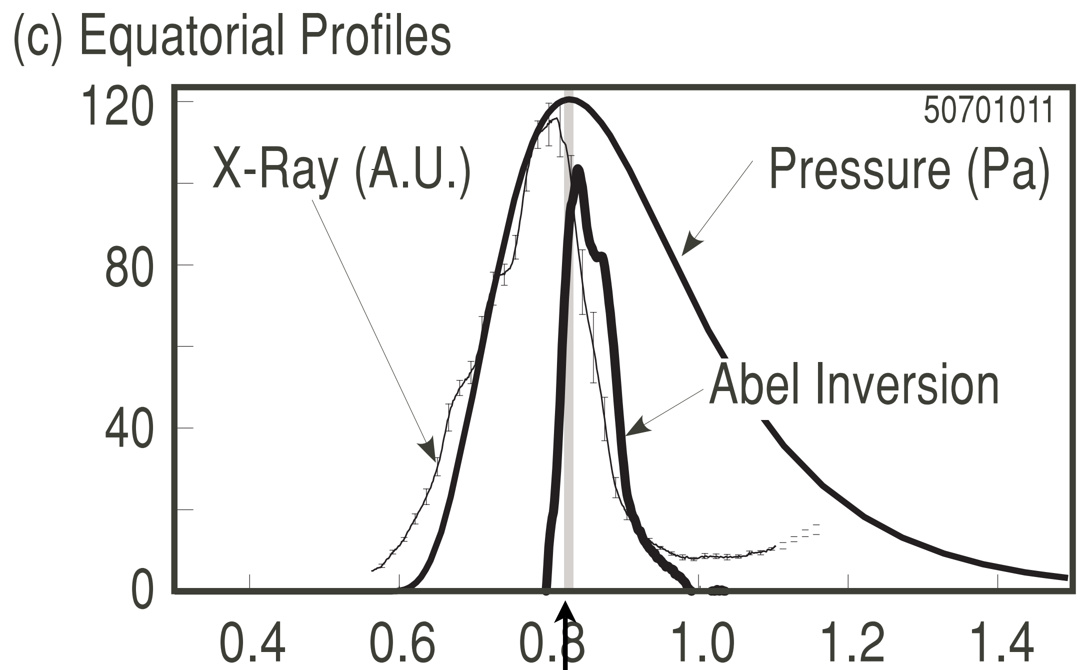

2.45 GHz
Resonance

“Best Fit” Anisotropic Equilibrium

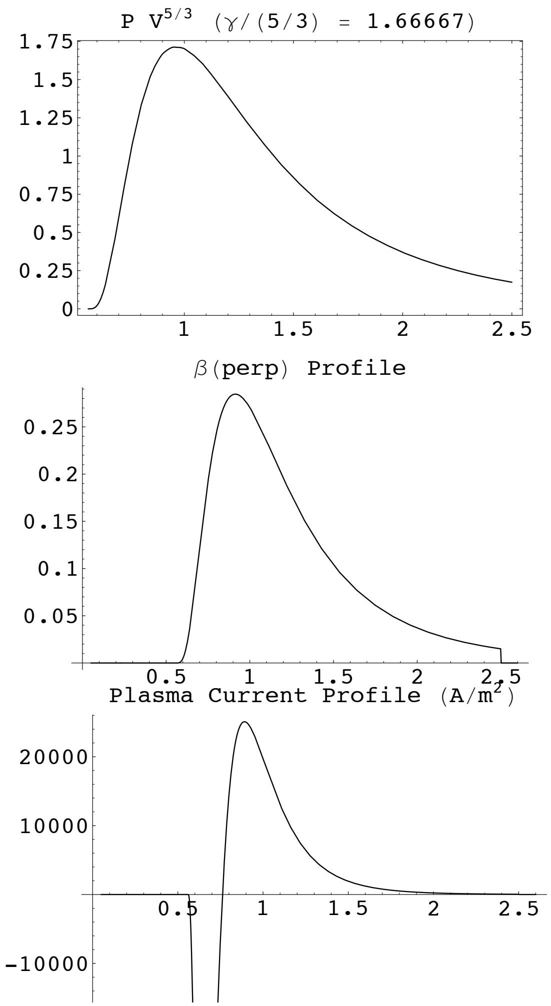

Peak pressure “in-between” 2.45 and 6.4 resonance.

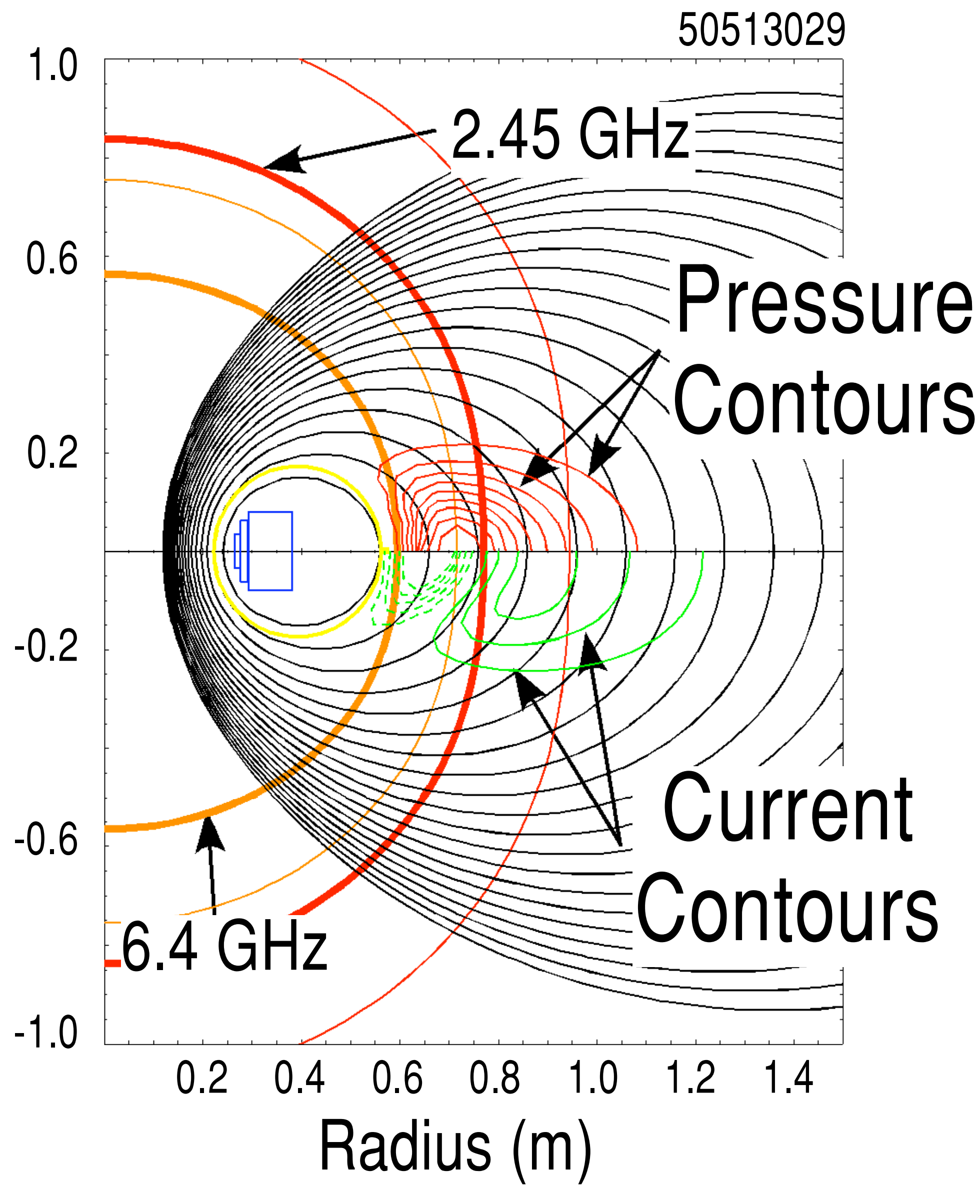

“Record” High Beta Discharge

Parameter	Fit Value	Fit Value	Fit Value
χ^2	15.1592	14.3351	14.5942
Ip	3817.59	3516.76	3356.57
δIf	-941.977	-794.85	-738.437
p	0	1	2
P(perp)/P(||)	1	3	5
R(peak)	0.716667	0.716667	0.716667
γ	1.66667	2.40741	2.40741
γ/(5/3)	1.	1.44444	1.44444
Press(Rpeak)	112.614	459.7	594.78
J Centroid	1.1976	1.19639	1.23389
Moment (A m^2)	6152.34	5207.42	5251.09
Max Perp β	0.137991	0.206572	0.267272
Perp β(Rpeak)	0.0218796	0.0893144	0.115559
Avg Perp β	0.070594	0.0354153	0.0383653
Plasma Volume	28.7984	28.7984	28.7984
Energy (J)	297.15	329.847	306.234
E/Ip (J/kA)	77.8369	93.7928	91.2342

Steep Gradient!

High β!

χ^2 Summary

2.45 GHz Only

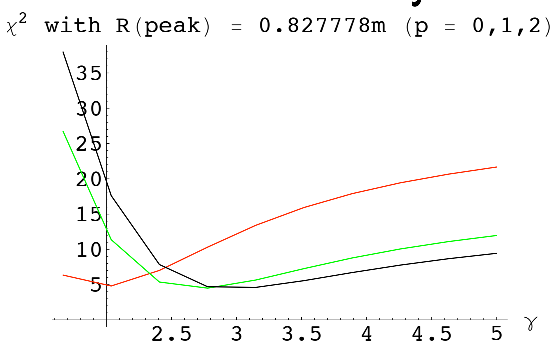

6.4 GHz Only

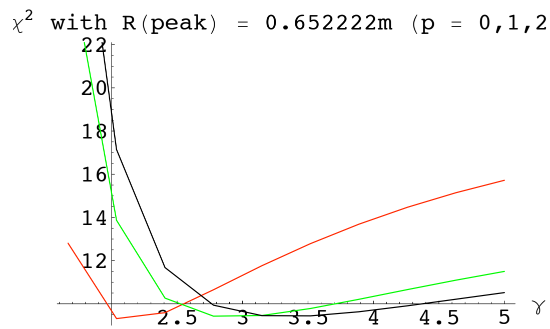

2.45 GHz & 6.4 GHz

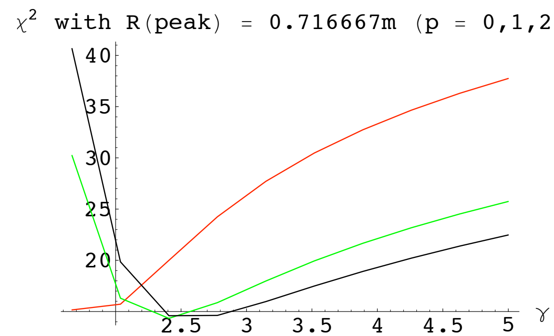

χ^2 increases as 6.4 GHz heating is applied.

χ^2 is lowest for 2.45 GHz only.

Measuring Multipoles

- The present LDX magnetic diagnostics are relatively far from the plasma diamagnetic current and from the floating-coil.
- In this case, equilibrium reconstruction is equivalent to least-squares fit between magnetic diagnostics and multipole moments.
- The plasma's dipole moment and the quadrupole moment formed from the inductively-reduced f-coil current dominate the far-field.

Examples

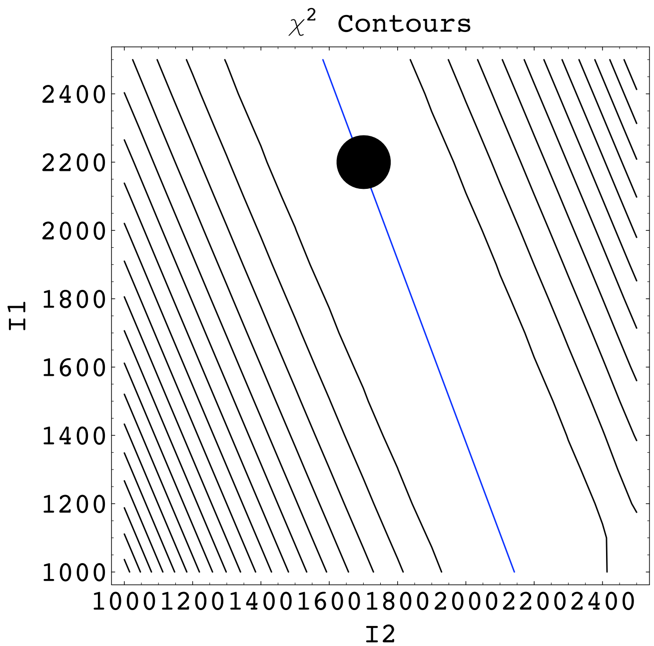

Figure 1: Contours of χ^2 for Shot 50318014 ($t = 3$ s) computed as the current within two fixed filaments are varied. The blue line represents the combination of currents producing a constant total dipole moment, $M_{tot} \propto 2960$ A·m^2. χ^2 is essentially constant along this line and increases rapidly to either side.

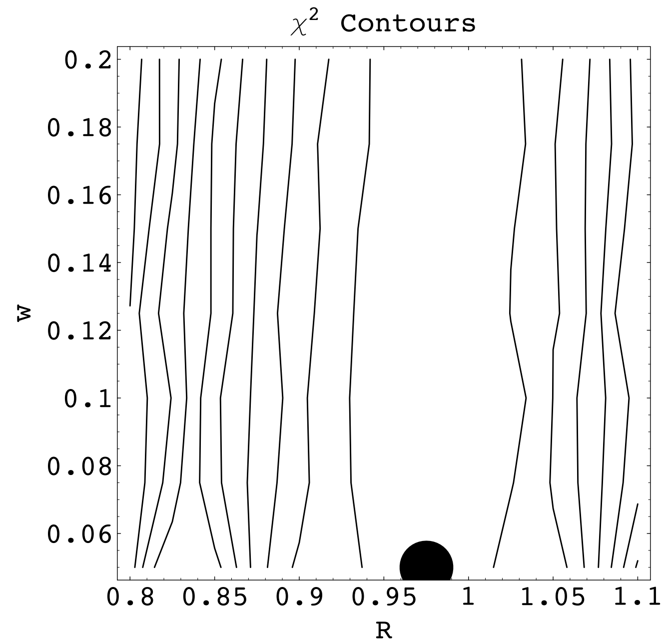

Figure 3: Contours of χ^2 for Shot 50318014 ($t = 3$ s) computed for a co-axial current ring with elliptical cross-section. For $R_c \sim 0.97$ m, the plasma dipole moment is equivalent to the best fit values computed in the previous section. The LDX magnetic diagnostics are unable to determine the width of the current channel.

Contours of equal χ^2 show a minimum for a given plasma dipole moment.

New Magnetic Diagnostics will be Closer to Plasma

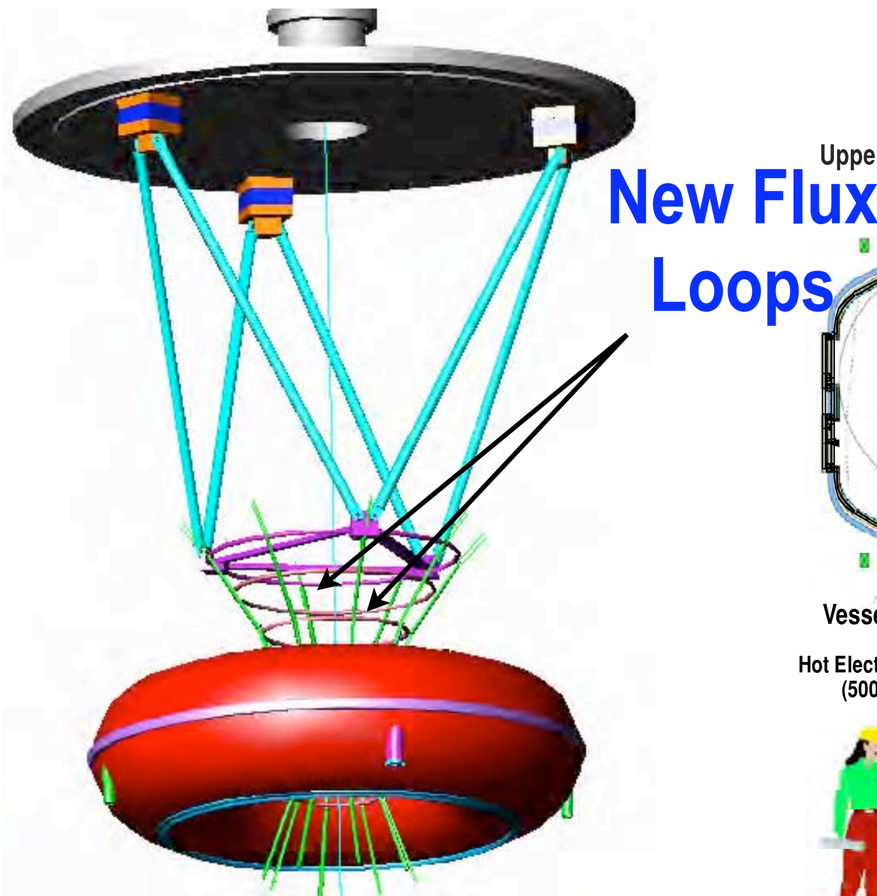

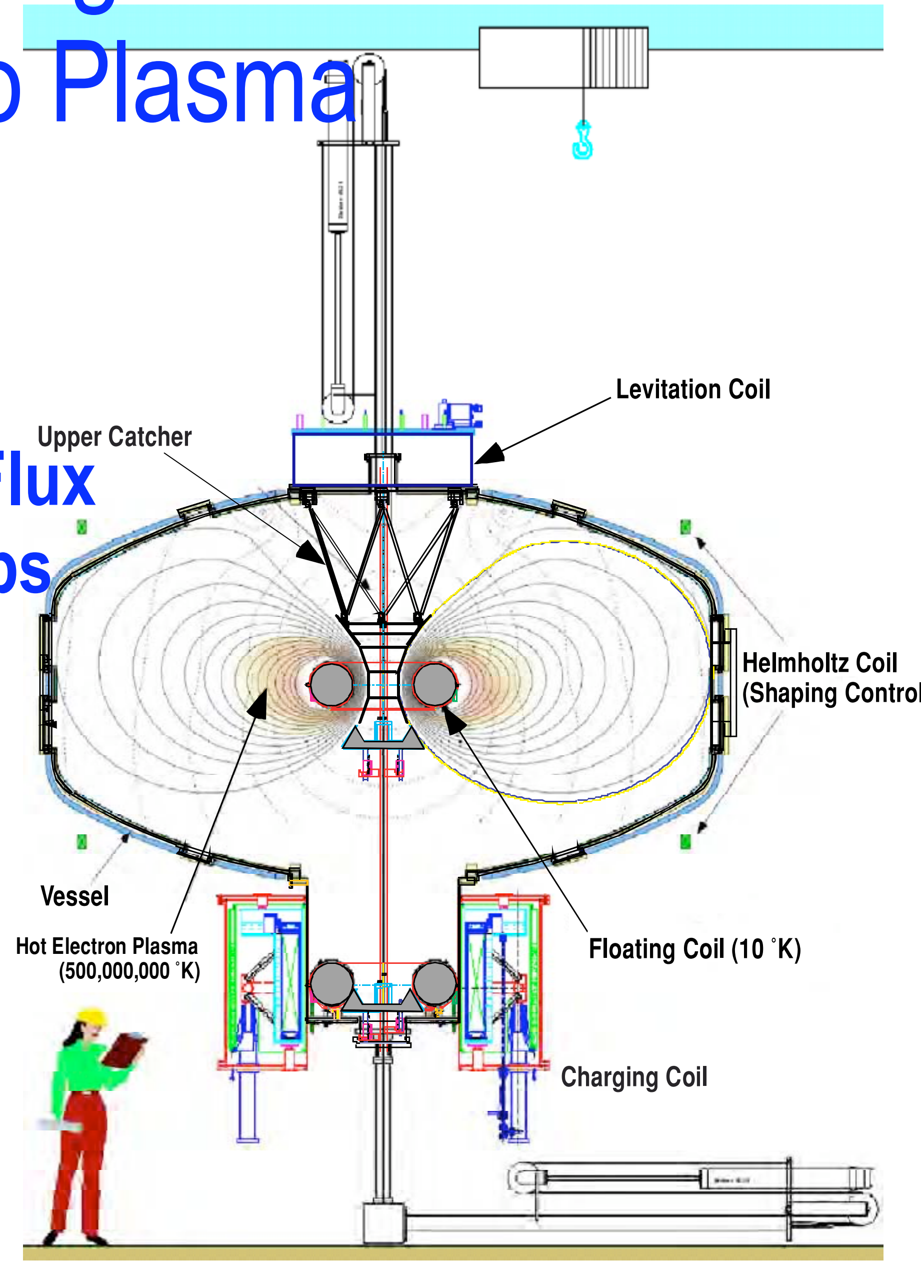

Summary

- Equilibrium reconstruction demonstrate that plasmas with high local beta are created in LDX
- X-ray images show the fast electrons to be localized at the ECRH resonance. The fast electrons are anisotropic.
- Anisotropic equilibria are well fit to magnetic measurements. The equilibria have pressure gradients that exceed the usual MHD instability limits.
- New magnetic diagnostics will be installed closer to the plasma to distinguish more details of the pressure profile.